Journal of
Intelligent Material
Systems and Structures

Original Article

Journal of Intelligent Material Systems and Structures
2014, Vol 25(3) 342–351

DOI: 10.1177/1045389X13494931
jim.sagepub.com
SAGE

Modeling and analysis of magnetorheological inner mass single unit impact dampers

Aref Afsharfard and Anooshiravan Farshidianfar

Abstract

In this article, ongoing studies to apply semi-active control devices to reduce undesired vibrations of civil engineering structures are investigated. In doing so, the barrier of the nonlinear inner mass single unit impact dampers is equipped by the magnetorheological fluid dampers. For convenience, this kind of impact dampers is briefly named smart impact dampers. Dynamic behavior of a vibratory system equipped with the smart impact damper is modeled based on the modified Bouc–Wen model for the magnetorheological damper. Performance of the smart impact damper to suppress free vibration of an Euler–Bernoulli beam is investigated. Furthermore, effects of varying applied current to the magnetorheological fluid damper on vibratory behavior of the beam are illustrated in user-oriented charts. The analysis results show that the smart impact dampers with optimal parameters can suppress undesired vibrations much better than conventional impact damper systems.

Keywords

Magnetorheological fluid damper, modified Bouc–Wen, smart impact damper, damping inclination

Introduction

Passive control devices, including base isolation, friction dampers, viscous fluid dampers, impact dampers, tuned mass dampers, and tuned liquid dampers, are accepted means for mitigating the effects of dynamic loadings (Soong and Spencer, 2002). Kwon et al. (1998) investigated the application of tuned mass dampers to control bridge vibration under moving loads. Marivani and Hamed (2009) presented a nonlinear, two-dimensional model to investigate the response of a structure equipped with a tuned liquid damper. An inner mass single unit impact damper (or simply "impact damper") is a small loose mass within a main mass. These systems can be extensively applied to attenuate the undesirable vibration of robot arms, turbine blades, and so on (Dimentberg and Iourtchenko, 2004; Zhang and Angeles, 2005). It is shown that in the neighborhood of the first and second resonances, the impact dampers would operate more efficiently than classical dampers (Blazejczyk-Okolewska, 2001). In the past few years, behavior of impact dampers has been investigated experimentally, analytically, and numerically (Afsharfard and Farshidianfar, 2012a, 2012b; Cheng and Wang, 2003; Cheng and Xu, 2006). Son et al. (2010) proposed active momentum exchange impact dampers to suppress the first large peak value of the acceleration response due to a shock load. Bapat and Sankar (1985) showed that the coefficient of restitution has a great effect on the performance of impact dampers. They demonstrated that in the case of single unit impact dampers, optimized parameters at resonance are not necessarily optimal at other frequencies. Cheng and Xu (2006) obtained a relation between coefficient of restitution and impact damping ratio. They showed that optimal initial displacement is a monotonically increasing function of damping.

Although the impact damper has been investigated for a longtime, there are still several shortcomings in this area of research that should be noted. Like other passive devices, impact dampers have the limitation of not being capable of adapting to varying usage patterns and loading conditions. The effects of using semi-active impact dampers are one of the important aspects, which need to be further investigated. The main thrust of this article lies in this subject.

Department of Mechanical Engineering, Ferdowsi University of Mashhad, Mashhad, Iran

Corresponding author:
Aref Afsharfard, Department of Mechanical Engineering, Ferdowsi University of Mashhad, Mashhad, Iran.
Email: Aref.Afsharfard@gmail.com

The magnetorheological (MR) fluids are suspensions that exhibit a rapid, reversible, and tunable transition from a free-flowing state to a semi-solid state upon the application of an external magnetic field (Wang and Liao, 2011). Applications of MR fluids in mechanical systems have been extensively investigated. The reason for this interest lies in the fact that MR fluids can provide a simple and rapid response interface between electronic controls and mechanical systems (Kordonsky, 1993). Wang et al. (2005) investigated vibratory behavior of tall building structures equipped with a semi-active tuned liquid damper with the MR fluids (magnetorheological tuned liquid column damper (MR-TLCD)). They showed that the MR-TLCDs can suppress undesired vibrations much better than conventional TLCD system. Dominguez et al. (2008) simulated the hysteresis behavior of the dampers using a nonlinear model based on the Bouc–Wen model. They considered frequency, amplitude, and current excitation as dependent variables in their investigation.

To take maximum advantage of MR fluids in control applications, a reliable method is needed to predict their nonlinear response. Several phenomenological models have been used to characterize the behavior of MR fluid dampers for seismic protection, vehicle applications, and so on (Kamath et al., 1996; Makris et al., 1996; Weber et al., 2008). Generally, most MR dampers have been analyzed using the Bingham model. This model accounts for MR fluid behavior beyond the yield point. However, it assumes that the fluid remains rigid in the pre-yield region. Thus, the Bingham model does not describe the fluid elastic properties at small deformations and low shear rates, which are necessary for dynamic applications (Kamath and Wereley, 1997; Lee et al., 2002). To overcome this shortcoming, Spencer et al. (1997) presented the so-called modified Bouc–Wen model. Behavior of the MR dampers can be accurately described using the current-dependent–modified Bouc–Wen model (Guglielmino, 2008; Yang et al., 2002).

The main goals of the present study are twofold: (1) to use the MR fluid dampers in the barriers of the passive nonlinear impact dampers. For convenience, this type of impact dampers is named "smart impact damper." (2) To investigate the application of the smart impact dampers for structural stability augmentation. To the best of our knowledge, there has been no consideration toward these issues up to now. It should be noted that in the smart impact dampers, properties of the barriers can easily be changed with varying the input current. As a result, it can be concluded that the smart impact dampers can be optimized without any mechanical change in their specification.

In the present study, a simple model of a passive single unit impact damper (or simply "conventional impact damper") is presented as a combination of nonlinear springs and viscose dampers. The nonlinear springs are used to describe the Hertzian contact between the impact mass and the main mass. The smart impact damper is modeled using the nonlinear springs and the MR fluid dampers. Application of the conventional impact dampers is compared with the smart impact dampers.

The dynamic behavior of the vibratory system (main mass) equipped with the conventional and smart impact dampers is described as explicit expressions. As a case study, application of the conventional impact damper and its equivalent smart impact damper for suppressing the free vibrations of an Euler–Bernoulli beam is studied. Effects of varying the applied current and the mass ratio on the damping inclination of the smart impact damper are studied. In doing so, two user-oriented charts are illustrated to show the variation of the damping inclination. Finally, application of the smart impact damper to improve the ability of vibration quenching is discussed.

Mathematical model of vibratory system

An impact damper is a mass placed inside the structure and holds a small gap (clearance) to the structure. When the displacement of the main system exceeds the clearance, the impact mass collides with the container wall (barrier) accompanying with energy dissipation and momentum exchange (Cheng and Xu, 2006). Consider an impact damper with impact mass m, gap size d, and oscillator with linear stiffness K, main mass M, and viscous damping C. Note that the mass ratio is defined as $\mu = m/M$. A free vibratory system equipped with the conventional and the smart impact damper is shown in Figure 1.

In Figure 1, variables x and y are the main mass and impact mass displacements, respectively. When $|y - x| < d/2$, the impact mass moves freely at a constant speed without causing any collision. Therefore, the governing differential equation of the main mass and impact mass motion can, respectively, be written as follows

$$M\ddot{x} + C\dot{x} + Kx = 0 \tag{1}$$

$$m\ddot{y} = 0 \tag{2}$$

In this article, the friction is neglected because the gap size is assumed very small. The above differential equation can be easily solved to formulate the displacements of the main mass between the impacts i and $i + 1$. As shown in Figure 1, it is clear that impacts occur only when the following holds

$$|x - y| = \frac{d}{2} \tag{3}$$

In the present study, the elastic behavior of the barriers is modeled using a nonlinear spring, which is used to describe the Hertzian contact force. Moreover, it is

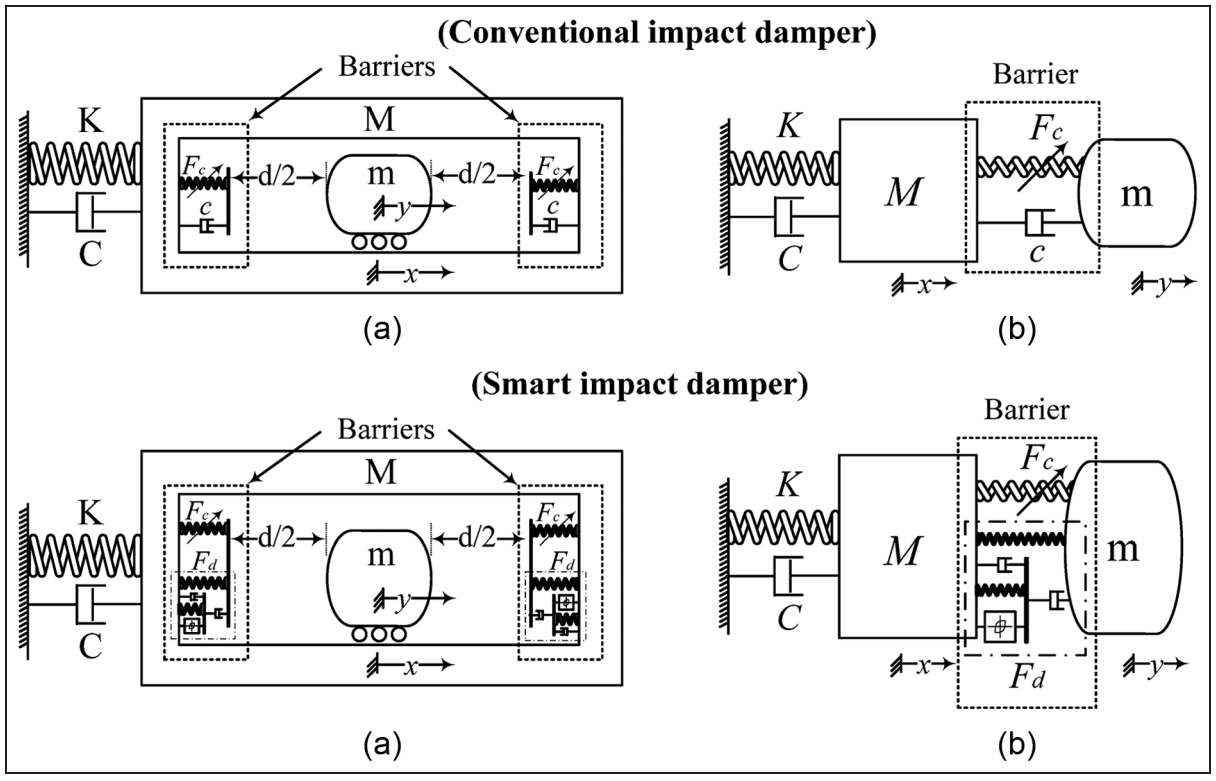

Figure 1. (a) Schematic model of the main vibratory system equipped with the conventional and smart impact dampers and (b) barriers of the conventional and smart impact dampers when contact occurs.

considered that the impact damper system does not have any effect on the impact condition. The expression for the contact force (F_c) can be written as follows

$$F_c = k(y-x)^{3/2} \tag{4}$$

where k is the barrier stiffness. Note that the contact force does not depend on the input current. Therefore, F_c is similar in both the smart and conventional impact dampers.

When the impact mass collides with the barriers ($|y-x| \geq d/2$), the schematic diagram of the vibratory system with smart and conventional impact damper is illustrated in Figure 1(b). The governing equation of the impact damper system, when contact occurs, can be written as follows

$$\begin{cases} M\ddot{x} + C\dot{x} + Kx = F_c + F_d \\ m\ddot{y} = -F_c - F_d \end{cases} \tag{5}$$

where F_d is damping force. In the case of conventional impact dampers, $F_d = c(\dot{y}-\dot{x})$. Therefore, the governing equation for a vibratory mass equipped with the conventional impact damper can be given by

$$\begin{cases} M\ddot{x} + C\dot{x} + Kx = k(y-x)^{3/2} + c(\dot{y}-\dot{x}) \\ m\ddot{y} = -k(y-x)^{3/2} - c(\dot{y}-\dot{x}) \end{cases} \tag{6}$$

Parameter estimation of MR damper using the modified Bouc–Wen model

In the present study, the MR fluid dampers are used at constant currents, since the modified Bouc–Wen model can be used to simulate them. The modified Bouc–Wen model is a mechanical model for MR fluid dampers based on the Bouc–Wen hysteresis model. Spencer et al. (1997) showed that the best results for portraying the hysteretic behavior of the MR fluid dampers can be obtained using the modified Bouc–Wen model. The schematic diagram of the modified Bouc–Wen fluid damper is shown in Figure 2.

The damping force in this model is given by (Spencer et al., 1997; Wang and Liao, 2011)

$$F_d = c_1\left(\dot{\psi}-\dot{x}\right) + k_1(y-x) \tag{7}$$

where k_1 is accumulator stiffness and c_1 is viscous damping for force roll-off, which is more significant at low relative velocities ($d(y-x)/dt$). Variable ψ can be calculated using the following relations (Spencer et al., 1997)

$$\begin{cases} \dot{\psi} = \frac{1}{c_0+c_1}\left[\alpha\phi + c_0\dot{y} + c_1\dot{x} + k_0(y-\psi)\right] \\ \dot{\phi} = -\gamma\phi\left|\dot{y}-\dot{\psi}\right||\phi|^{n-1} - \beta\left(\dot{y}-\dot{\psi}\right)|\phi|^n + \delta\left(\dot{y}-\dot{\psi}\right) \end{cases} \tag{8}$$

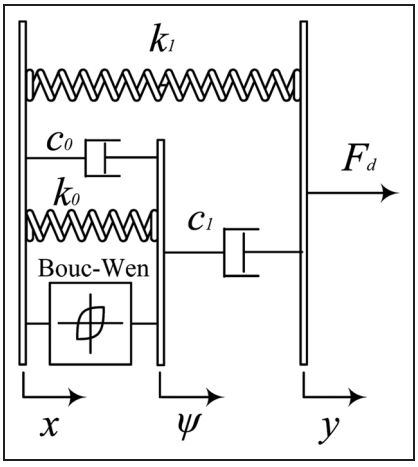

Figure 2. Modified Bouc–Wen model of MR fluid damper (Spencer et al., 1997).
MR: magnetorheological.

Table 1. Parameters of the MR fluid damper (Giuclea et al., 2004; Guglielmino, 2008).

u (A)	c_0 (N s/m)	c_1 (N s/m)	α (N/m)	k_0 (N/m)
0.02	121	10,300	2950	527
0.06	340	8350	15,300	306
0.10	465	13,900	23,900	22.3
0.20	966	33,600	34,000	468
0.40	1690	83,900	58,500	988
0.60	2880	93,300	89,800	1990
0.80	3220	10,1800	104,900	1240
1.05	3500	10,7800	114,500	1330
1.45	4730	111,600	114,400	1630
1.75	4050	122,500	133,900	2010

MR: magnetorheological.

In the above relation, c_0 is viscous damping at large relative velocities and k_0 is stiffness at large relative velocities. In the present study, it should be noted that both two sides of the MR fluid damper are considered moveable. In other words, the MR fluid damper can be connected to a fixed body ($\Delta x = 0$) or movable body ($\Delta x \neq 0$). Therefore, the presented modified Bouc–Wen model can be used to describe the behavior of the MR fluid dampers, which are connected to the movable main mass. Hence, when contact occurs ($|y - x| \geq d/2$), the equations of motion for the smart impact damper system, regarding the modified Bouc–Wen model, are as follows

$$\begin{cases} M\ddot{x} + C\dot{x} + Kx = k(y-x)^{3/2} + c_1(\dot{\psi} - \dot{x}) + k_1(y-x) \\ m\ddot{y} = -k(y-x)^{3/2} - c_1(\dot{\psi} - \dot{x}) - k_1(y-x) \end{cases} \tag{9}$$

where n, γ, β, δ, k_1, α, c_0, c_1, and k_0 are coefficients of the MR fluid damper model.

Numerical simulation

Properties of the MR fluid damper

The following values are selected for the fixed coefficients of the model: $n = 2$, $\gamma = 50{,}000\ \mathrm{m}^{-2}$, $\beta = 613{,}000\ \mathrm{m}^{-2}$, $\delta = 30.56$, and $k_1 = 540$ N/m. Since the fluid yield stress is dependent on input current (u), parameters α, c_0, c_1, and k_0 can be assumed as a function of the input current. These parameters of the MR fluid damper, corresponds to the studies of Giuclea et al. (2004) and Guglielmino (2008), are given in Table 1.

Vibratory properties of the main system

In this section, vibratory behavior of an Euler–Bernoulli beam, which is equipped with the presented impact dampers, is investigated. Schematic diagram of the beam and its properties is shown in Figure 3.

To increase effectiveness, the impact dampers should be installed in part of the main system, which

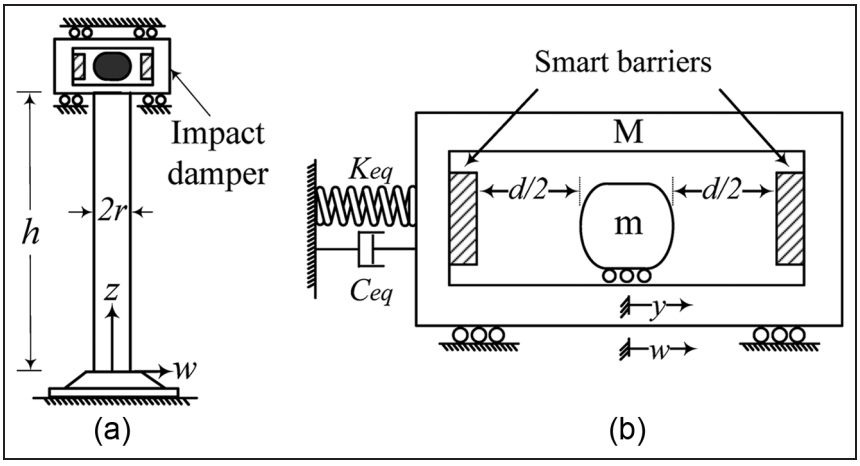

Figure 3. (a) Schematic diagram of the beam with the smart impact damper and (b) schematic diagram of the equivalent smart vibro-impact system.

maximally vibrates. As shown in Figure 3, the smart impact damper is installed in the beam tip. The equation of motion for the Euler–Bernoulli beam system can conveniently be formulated using the principle of virtual work (Clough and Penzien, 2010; Simitses and Hodges, 2006). This principle requires that the external virtual work (δW_E) be equated to the internal virtual work (δW_I). Using the Euler–Bernoulli assumptions, the external and internal virtual works can be given by

$$\delta W_E = \int_0^h \rho A \frac{\partial^2 w(z,t)}{\partial t^2} \delta w(z,t) dz \tag{10}$$

$$\delta W_I = \int_0^h EI \left\{ \frac{\partial^2 w(z,t)}{\partial z^2} + a_1 \frac{\partial^2}{\partial z^2} \left(\frac{\partial w(z,t)}{\partial t} \right) \right\} \delta \left(\frac{\partial^2 w(z,t)}{\partial z^2} \right) dz \tag{11}$$

where w is deflection of the piers, A is the cross-sectional area of the piers, and a_1 is a damping constant. Based on the separation of variable method, deflection of the piers can be written as follows

$$w(z,t) = \eta(z)\, q(t) \tag{12}$$

where $\eta(z)$ is the shape function and $q(t)$ is time-dependent response. Substituting the above relation into equations (10) and (11) and equating the external virtual work to the internal virtual work result in

$$\left(\int_0^h \rho A \eta^2 \, dz \right) \frac{d^2 q}{dt^2} + \left(\int_0^h EI a_1 \left(\frac{d^2 \eta}{dz^2} \right)^2 dz \right) \frac{dq}{dt} + \left(\int_0^h EI \left(\frac{d^2 \eta}{dz^2} \right)^2 dz \right) q = 0 \tag{13}$$

Using the above relation, the equivalent mass, damping, and stiffness of the beam can be approximated. For the first mode shape of vibration ($\eta(z) = 0.5 - 0.5 \cos(\pi z/h)$), the dynamic properties of the main vibratory system (the beam) can be calculated as $M_{eq} = 0.3750 \rho A h$ and $C_{eq} = 12.1761 a_1 EI/h^3$ and $K_{eq} = 12.1761 EI/h^3$. In the present study, the elastic modulus and mass density of the beam are considered to be $E = 200$ GPa and $\rho = 7800$ kg/m^3, respectively (Beer et al., 2006). Therefore, the nominal values of the main vibratory system parameters, if $h = 11.1$ m, $r = 0.72$ m, and $a_1 = 9 \times 10^{-4}$ s, are equal to $M = 52794.8$ kg, $C = 68003.2$ N s/m, and $K = 752827947.4$ N/m. The barrier stiffness (k) is assumed to be 67.1 MN/m.

Result and discussion

In the smart impact dampers, momentum exchange between the colliding masses (during the contact of the impact mass with the barriers) can be controlled using the MR fluid damper in the barriers. During the collision, the contact force (F_c) varies with the relative displacement of colliding bodies ($y-x$). Therefore, the contact force cannot be controlled with external parameters (e.g. input current). Unlike the contact force, the so-called damping force (F_d), in the smart impact dampers, is variable with the input current. Therefore, the damping force can be controlled externally regarding the contact parameters. In this section, effects of the input current on performance of the smart impact dampers are investigated.

In the present study, the governing differential equation of the main mass and impact mass motions is presented when the impact mass freely moves between the barriers. It is shown that if the relative motion of masses exceeds than half of the gap size, the impact occurs. Using the mass ratio, stiffness, and damping behavior of the barriers, equation of motion for the colliding masses, in the smart and conventional impact dampers, is theoretically presented.

Many contacts may occur between the masses during the oscillations of the vibratory system equipped with the impact damper. In each of the collisions, the equation of motion for the colliding masses should be solved. In order to evaluate the performance characteristics of the smart and conventional impact dampers, computer simulation is done in MATLAB software. In the present study, the nonlinear differential equations are solved using the Newmark-beta integration method (Afsharfard and Farshidianfar, 2012b), and the time step is considered as $\Delta t = 10^{-4}$ s.

The modified Bouc–Wen model is used to predict the force generated by the MR fluid damper. The response of the MR fluid damper, which is used in the barrier of the smart impact damper system due to initial contact velocity of 70 cm/s for constant current of 0.02 A, is shown in Figure 4.

As shown in Figure 1, vibratory behavior of the colliding masses in the conventional impact dampers is described using springs and viscose dampers. For comparing the smart impact damper with the conventional impact damper, an equivalent viscose damping coefficient should be calculated for the viscose dampers. To find the equivalent viscose damping coefficient, variation of the damping force (F_d) with the relative velocity ($d(y-x)/dt$) is estimated with a linear approximation. Slope of the approximated line is used as the viscose damping coefficient (c). In Figure 5, waveforms of free vibrations of the discussed beam equipped the smart and the conventional impact dampers are compared with the system without impact damper.

For the linear systems equipped the impact dampers, the decay of maximum displacement is initially linear, and after a considerable decrease in displacement amplitude, it is exponential (Bapat and Sankar, 1985). The slope of trend line passes through the initial

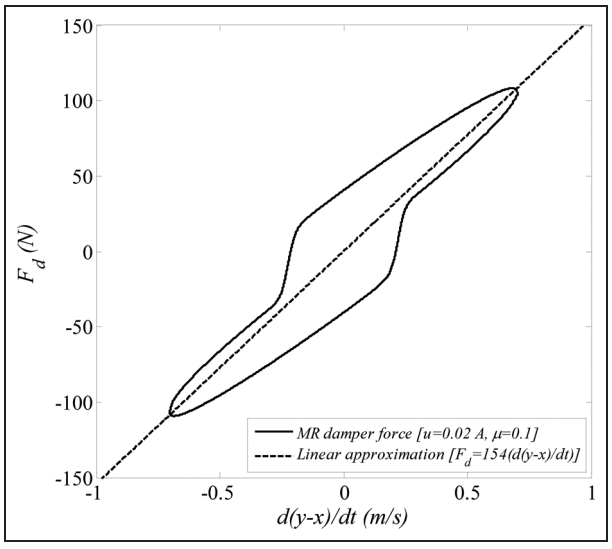

Figure 4. Force–velocity loop for the MR damper in the smart impact damper system.
MR: magnetorheological.

maximum displacements of the main vibratory system can be considered as an appropriate and simple parameter to show the speed of vibration suppression by the impact dampers. This parameter is usually represented by a term named damping inclination (DI), defined as follows

$$DI = \frac{X_1 - X_2}{t_2 - t_1} \tag{14}$$

where t_1 and t_2 are the times of occurrence of the maximum positive displacements X_1 and X_2, respectively. In Figure 5, for the vibratory system equipped the conventional and the smart impact dampers, the damping inclinations are equal to 0.1570 and 0.1998 m/s, respectively. Therefore, it can be concluded that application of the smart impact damper to suppress initial vibration of the presented beam is more than 27% stronger or faster than the conventional impact damper.

In inelastic collisions, some kinetic energy is transformed into heat, sound, and other forms of energy. Ability of impact dampers to suppress undesired vibration depends on the amount of energy loss in the collision of the impact mass with the barrier. The restitution coefficient (R) is proportional to the loss of energy during the collision (Ibrahim, 2009). The restitution coefficient is defined as follows

$$R = \frac{\left(\frac{d(y-x)}{dt}\right)_+}{\left(\frac{d(y-x)}{dt}\right)_-} \tag{15}$$

where the subscripts " + " and "−" present the values of variables at, just after, and just before the collision. Note that dissipation of energy is high in low amounts of the restitution coefficients. In perfectly elastic collisions, $R = 1$ (no energy loss), and in perfectly plastic collisions, $R = 0$.

Variation of the restitution coefficient versus time in the vibratory system with the conventional impact damper and the smart impact damper is illustrated in

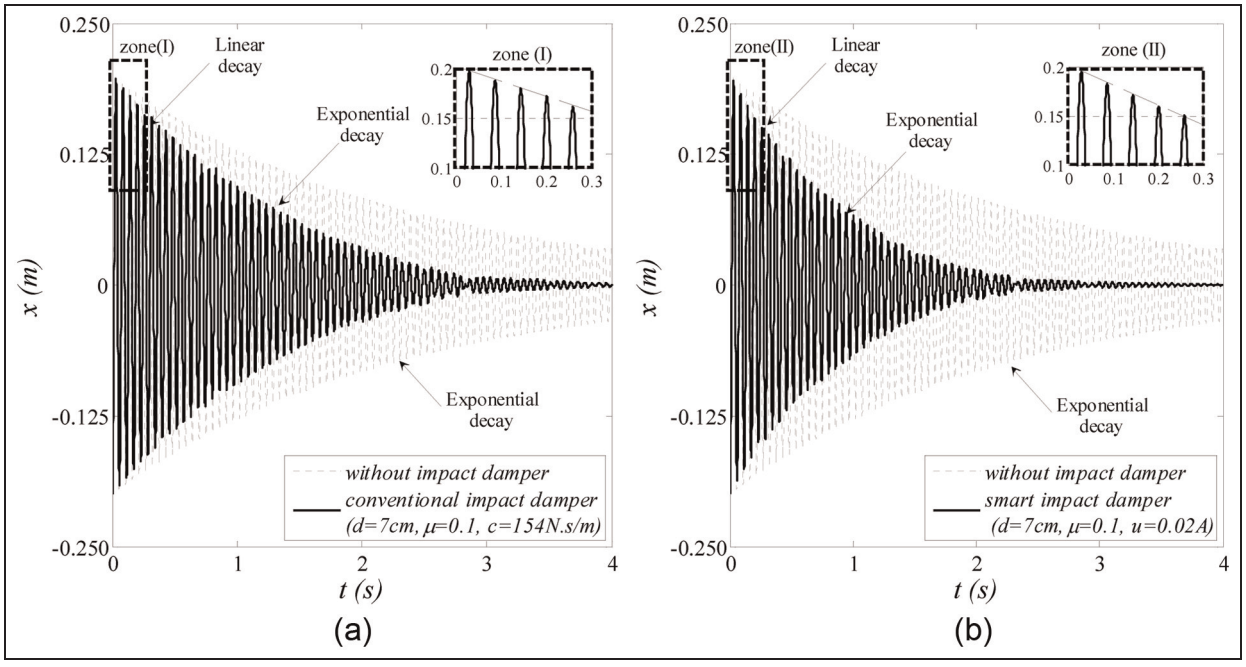

Figure 5. Waveforms of the beam vibrations without impact damper and (a) with the conventional impact damper and (b) the smart impact damper.

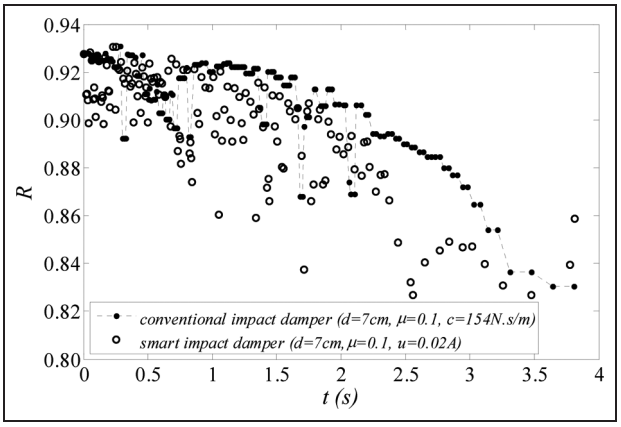

Figure 6. Variation of the restitution coefficient versus time in the conventional and the smart impact dampers.

Figure 6. Average of the restitution coefficients for the vibro-impact system with the smart impact damper and the conventional impact damper is equal to 0.8973 and 0.9080, respectively. As a result, it can be concluded that the smart impact damper can dissipate undesired energy better than the conventional impact damper. Therefore, the smart impact damper works better than the convention impact damper.

In the case of the smart impact damper, which is presented in this study, the gap size is small and the impact mass cannot move in the gap distance with high speed. Therefore, the impact mass cannot exchange enough momentum through the contact with the main mass unless the impact mass is heavy enough. Since the behavior of the MR fluid dampers is dependent on input current, performance of the smart impact dampers is variable with input current. Variations of the damping inclination versus the input current, gap size, and mass ratio are illustrated in Figures 7 and 8.

As it was mentioned before, dependence of the barrier behavior on electrical input current is the main property of the presented smart impact damper. In other words, application of the smart impact dampers can be improved without any mechanical change in their specification. This property can clearly be observed in Figures 7 and 8. For example, in Figure 7, it is shown that for the smart impact damper with $\mu = 0.07$ and $d = 5$ cm, the damping inclinations are equal to 0.1697 and 0.2195 m/s if the input currents are equal to 0.02 and 0.60 A, respectively. Therefore, the damping inclination can be improved more than 29% only by changing the input current. Two points 1 and 2 are specified in Figures 7 and 8, respectively. The damping inclinations for smart impact damper in points 1 and 2 are equal to 0.2195 and 0.1188 m/s, respectively. Furthermore, average of the restitution coefficients for smart impact damper in points 1 and 2 is equal to 0.9037 and 0.9693, respectively. Therefore, the smart impact damper in point 1 should be stronger than smart impact damper in point 2. Effect of using the smart impact dampers (with properties of points 1 and 2) on the main mass vibrations is shown in Figure 9. Finally, it can be concluded that selecting appropriate values for the input current, mass ratio, and gap size for the smart impact damper can increase the damping inclination and average of the restitution coefficient more than 84% and 7%, respectively.

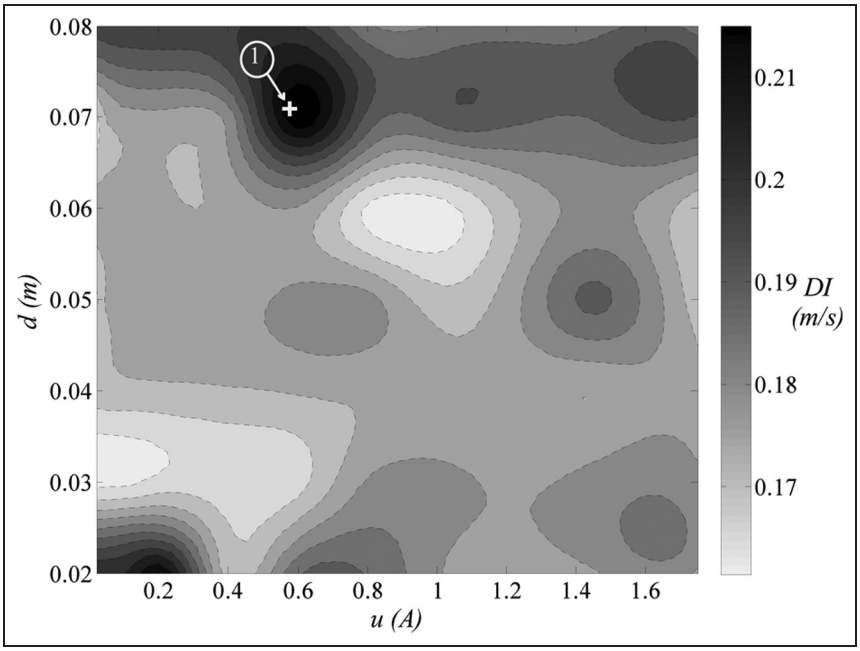

Figure 7. Variations of the damping inclination versus the input current and gap size (μ = 0.1).

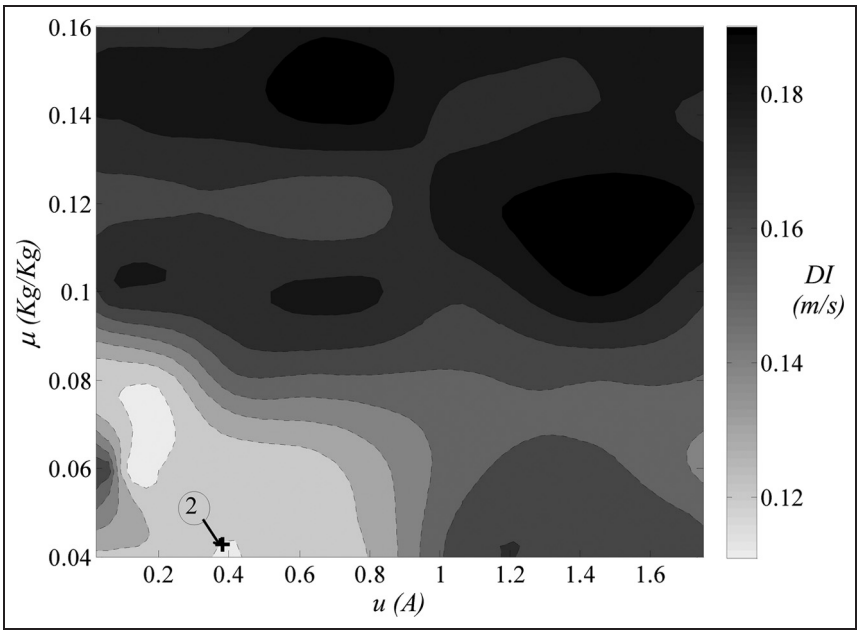

Figure 8. Variations of the damping inclination versus the input current and mass ratio (d = 5 cm).

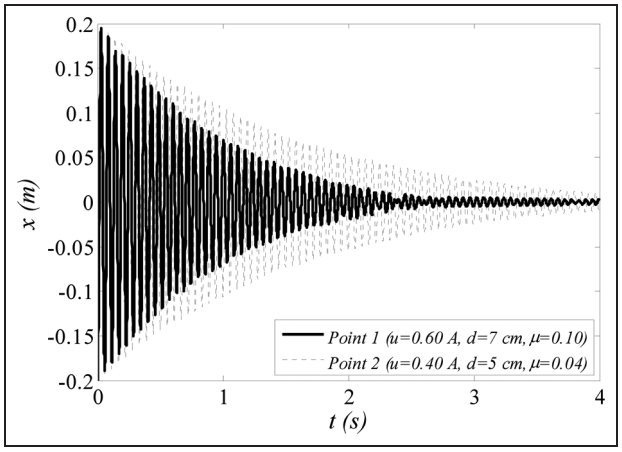

Figure 9. Waveforms of the beam vibrations with smart impact dampers in points 1 and 2.

Conclusion

The MR fluid dampers provide a level of technology that has enabled effective semi-active control in a number of practical applications. In the present study, the MR fluid dampers are used to improve the performance of the barriers in the inner mass single unit impact dampers. In the presented model of the impact damper system, the barrier consists of a nonlinear spring and a MR fluid damper. The nonlinear spring and MR fluid damper are used to show the elastic and damping behaviors of the barriers, respectively. The modified Bouc–Wen model is used to obtain the damping force of the MR fluid damper.

In this study, effect of applying the smart impact damper to suppress undesired vibration of an Euler–Bernoulli is investigated. It is shown that using a smart damper instead passive (conventional) impact damper can increase the damping inclination of the beam more than 27%. Furthermore, it is shown that average of the energy loss in the barrier of the smart impact damper is higher than the conventional impact damper.

Improving application of the smart impact dampers without any mechanical change in their specification is discussed. It is shown that changing the input current, without any mechanical optimization, can increase the damping inclination more than 29%.

Effects of varying the input current, the mass ratio, and the gap size on the performance of the smart damper are illustrated in two user-oriented charts. It is shown that selecting an appropriate input current, mass ratio, and gap size can increase the damping inclination more than 84%. Moreover, it is shown that selecting proper parameters leads to improve the average of the restitution coefficient more than 7.2%.

Declaration of conflicting interests

The authors declare that there is no conflict of interest.

Funding

This research received no specific grant from any funding agency in the public, commercial, or not-for-profit sectors.

References

Afsharfard A and Farshidianfar A (2012a) Design of nonlinear impact dampers based on acoustic and damping

behavior. *International Journal of Mechanical Sciences* 65(1): 125–133.
Afsharfard A and Farshidianfar A (2012b) An efficient method to solve the strongly coupled nonlinear differential equations of impact dampers. *Archive of Applied Mechanics* 82(7): 977–984.
Bapat CN and Sankar S (1985) Single unit impact damper in free and forced vibration. *Journal of Sound and Vibration* 99(1): 85–94.
Beer FP, Johnston ER, et al. (2006) *Mechanics of Materials*. Boston, MA: McGraw-Hill Higher Education.
Blazejczyk-Okolewska B (2001) Analysis of an impact damper of vibrations. *Chaos, Solitons & Fractals* 12(11): 1983–1988.
Cheng CC and Wang JY (2003) Free vibration analysis of a resilient impact damper. *International Journal of Mechanical Sciences* 45(4): 589–604.
Cheng J and Xu H (2006) Inner mass impact damper for attenuating structure vibration. *International Journal of Solids and Structures* 43(17): 5355–5369.
Clough RW and Penzien J (2010) *Dynamics of Structures*. Berkeley, CA: Computers and Structures.
Dimentberg MF and Iourtchenko DV (2004) Random vibrations with impacts. A review. *Nonlinear Dynamics* 36(2): 229–254.
Dominguez A, Sedaghati R and Stiharu I (2008) Modeling and application of MR dampers in semi-adaptive structures. *Computers & Structures* 86(3–5): 407–415.
Giuclea M, Sireteanu T, Stancioiu D, et al. (2004) Model parameter identification for vehicle vibration control with magnetorheological dampers using computational intelligence methods. *Proc IMechE, Part I: J Systems and Control Engineering* 218(7): 569–581.
Guglielmino E (2008) *Semi-Active Suspension Control: Improved Vehicle Ride and Road Friendliness*. London: Springer.
Ibrahim RA (2009) *Vibro-Impact Dynamics: Modeling, Mapping and Applications*. Berlin: Springer Verlag.
Kamath GM and Wereley NM (1997) A nonlinear viscoelastic-plastic model for electrorheological fluids. *Smart Materials and Structures* 6(3): 351.
Kamath GM, Hurt MK and Wereley NM (1996) Analysis and testing of Bingham plastic behavior in semi-active electrorheological fluid dampers. *Smart Materials and Structures* 5(5): 576.
Kordonsky WI (1993) Magnetorheological effect as a base of new devices and technologies. *Journal of Magnetism and Magnetic Materials* 122(1–3): 395–398.
Kwon H-C, Kim M-C and Lee I-W (1998) Vibration control of bridges under moving loads. *Computers & Structures* 66(4): 473–480.
Lee D-Y, Choi Y-T and Wereley NM (2002) Performance analysis of ER/MR impact damper systems using Herschel-Bulkley model. *Journal of Intelligent Material Systems and Structures* 13(7–8): 525–531.
Makris N, Burton SA, Hill D, et al. (1996) Analysis and design of ER damper for seismic protection of structures. *Journal of Engineering Mechanics* 122(10): 1003–1011.
Marivani M and Hamed MS (2009) Numerical simulation of structure response outfitted with a tuned liquid damper. *Computers & Structures* 87(17–18): 1154–1165.
Simitses GJ and Hodges DH (2006) *Fundamentals of Structural Stability*. Amsterdam; Boston, MA: Elsevier/Butterworth-Heinemann.
Son L, Hara S, Yamada K, et al. (2010) Experiment of shock vibration control using active momentum exchange impact damper. *Journal of Vibration and Control* 16(1): 49–64.
Soong TT and Spencer BF Jr (2002) Supplemental energy dissipation: state-of-the-art and state-of-the-practice. *Engineering Structures* 24(3): 243–259.
Spencer BF Jr, Dyke SJ, Sain MK, et al. (1997) Phenomenological model for magnetorheological dampers. *Journal of Engineering Mechanics* 123(3): 230–238.
Wang DH and Liao WH (2011) Magnetorheological fluid dampers: a review of parametric modelling. *Smart Materials and Structures* 20(2): 023001.
Wang JY, Ni YQ, Ko JM, et al. (2005) Magneto-rheological tuned liquid column dampers (MR-TLCDs) for vibration mitigation of tall buildings: modelling and analysis of open-loop control. *Computers & Structures* 83(25–26): 2023–2034.
Weber F, Feltrin G and Distl H (2008) Detailed analysis and modeling of MR dampers at zero current. *Structural Engineering and Mechanics* 30(6): 787–790.
Yang G, Spencer BF Jr, Carlson JD, et al. (2002) Large-scale MR fluid dampers: modeling and dynamic performance considerations. *Engineering Structures* 24(3): 309–323.
Zhang D-G and Angeles J (2005) Impact dynamics of flexible-joint robots. *Computers & Structures* 83(1): 25–33.

Appendix I

Notation

a_1	damping constant
A	cross-sectional area of the piers
c_0	viscous damping at large velocities
c_1	viscous damping for force roll-off at low velocities
C	viscous damping
d	gap size
DI	damping inclination
E	elastic modulus
F_c	contact force
F_d	damping force
h	beam length
I	moment of inertia
k	barrier stiffness
k_0	stiffness at large velocities
k_1	accumulator stiffness
K	linear stiffness
m	impact mass
M	main mass
q	time-dependent response
r	beam radius
R	restitution coefficient
u	input current
w	deflection of the pier
x	main mass displacement
y	impact mass displacement

z	distance to the clamped boundary of the pier
δW_E	external virtual work
δW_I	internal virtual work
Δ	variation
η	uniform vibration mode shape
μ	mass ratio
v	Poisson's ratio
ρ	mass density